Microporous and Mesoporous Materials 245 (2017) 45–50

Contents lists available at ScienceDirect

Microporous and Mesoporous Materials

journal homepage: www.elsevier.com/locate/micromeso

Short communication

# Distribution of open sites in Sn-Beta zeolite

Tyler R. Josephson, Glen R. Jenness, Dionisios G. Vlachos, Stavros Caratzoulas*

[a] Catalysis Center for Energy Innovation, University of Delaware, 221 Academy Street, Newark, DE, 19716, USA

ARTICLE INFO

*Article history:*
Received 27 November 2016
Received in revised form
20 January 2017
Accepted 20 February 2017
Available online 24 February 2017

*Keywords:*
Sn-Beta zeolite
Periodic DFT
Adsorption
$NH_3$
Pyridine
Acetonitrile

ABSTRACT

A survey of the open site geometries in Sn-Beta has been completed. Comparing the relative energies of 144 distinct open site structures identifies both T9 and T1 sites as the most stable open sites. However, a key feature of these sites is that the Sn-O-Si bridge which is hydrolyzed is opposite the SnOH, rather than adjacent. This results in geometries in which the SiOH in the open site is significantly more acidic than a surface SiOH or a SiOH defect in the zeolite, as found in adsorption calculations of $NH_3$, pyridine, and acetonitrile. Frequency shifts calculated for acetonitrile are consistent with experimental frequency shifts, and the proposed open site geometry suggests a new assignment for a peak observed experimentally by Harris et al. [1] and Otomo et al. [2] The stabilization of the open site silanol by the nearby Sn generates this unusual Brønsted acidity in the Sn-Beta open site, which highlights the need to consider new reaction mechanisms in the Sn-Beta literature.

© 2017 Elsevier Inc. All rights reserved.

## 1. Introduction

Sn-substituted zeolites have found applications in a wide range of carbonyl-activating chemistries, including Baeyer-Villiger oxidation of ketones to lactones [3], Meerwein-Ponndorf-Verley (MPV) reduction of carbonyls [4], 1,2-H-shift of glucose [5] and xylose [6], retro-aldol and esterification of sugars to lactates [7,8], the 1,2-carbon shift of glucose [9] and arabinose [10], dehydration reactions in the production of renewable aromatics from furans [11], and the catalytic transfer hydrogenation and etherification of 5-hydroxymethylfurfural [12]. Sn-Beta is particularly relevant for converting biomass derivatives derived from sugars – $C_5$ and $C_6$ compounds that are accommodated by its 12-member ring pores.

Several techniques have been employed to characterize the structure, activity, and selectivity of the active sites in Sn-Beta. Experiments with $^{119}Sn$ NMR on isotopically-enriched catalysts identified two distinct Sn sites: the closed site $Sn(OSi)_4$ and a hydrolyzed open site $Sn(OSi)_3OH$ [3,13,14]. Infrared spectroscopy of adsorbed $CD_3CN$ has been used to quantify the relative amounts of open and closed sites [1,2,14,15]. Boronat et al. identified a correlation between the amount of $CD_3CN$ adsorbed to open sites in different Sn-Beta samples and the zeolite activity for Baeyer-Villiger Oxidation, providing evidence for open sites as the active sites [15]. Bermejo-Deval et al. showed that $Na^+$-exchange of Sn-Beta shifts glucose selectivity from fructose to mannose, shutting down the intramolecular 1,2-H-shift and activating the intramolecular 1,2-C-shift. In addition, $NH_3$ adsorption shuts down catalyst activity by blocking open sites [14]. Otomo et al. identified weak Brønsted acidic silanols in Sn-Beta using IR spectroscopy of adsorbed $CD_3CN$, and showed that $Li^+$-, $Na^+$-, and $NH_4^+$-exchange passivates these silanols and reduces side reactions in Baeyer-Villiger Oxidation [2]. Recently, Harris, et al. demonstrated the use of pyridine as a selective titrant for these open sites, demonstrating a concomitant reduction in turn-over-frequency for glucose isomerization as open sites are blocked by increasing amounts of pyridine adsorption [1]. Brønsted acids have been hypothesized in Sn-Beta due to its activity in etherification [12], however pyridine adsorption has not given evidence of Brønsted acids in Sn-, Zr-, or Ti-Beta [16,17].

Because individual Sn-Beta active sites are difficult to isolate and test in experiment, the Davis group has synthesized and tested silsesquioxane models of the Sn-Beta active sites [18,19]. These have shown that while the open site model catalysts are significantly more active, the closed site model does have a small amount of glucose isomerization activity. However, the acac ligands present on the open site models stabilize the C-shift reaction [39], and several differences between the heterogeneous and homogeneous systems, including solvent and confinement effects, conflated the comparison with Sn-Beta.

* Corresponding author.
*E-mail address:* cstavros@udel.edu (S. Caratzoulas).

http://dx.doi.org/10.1016/j.micromeso.2017.02.065
1387-1811/© 2017 Elsevier Inc. All rights reserved.

To attribute $\nu$(C≡N) = 2316 $cm^{-1}$ to the open site, and $\nu$(C≡N) = 2308 $cm^{-1}$ to the closed site, Boronat, et al. also performed DFT calculations using cluster models of Sn-Beta with Sn substituted at the T1, T5, and T9 sites. [1]Both T5 and T9 open sites gave comparable $\nu$(C≡N) shifts to experimental $\nu$(C≡N) shifts, and all open sites more strongly bound $CH_3CN$ than the closed sites [15]. Shetty, et al. and Yang, et al. have used periodic DFT to compare the relative stability of the Sn substitution at all nine T sites, finding T2 to be most stable [20,40] for closed sites—but open sites were not investigated. Also in the same year, Bare et al. used X-ray absorption fine structure (EXAFS) to characterize Sn-Beta, concluding that Sn is substituted as pairs into the T1 and T2 positions [21]. Since then, a number of theoretical mechanistic studies have used the T2 site [22,23], the T7 site [24,25], or T9 site [26] in investigations of the mechanism for glucose isomerization.

However, no systematic study of the relative stability of Sn-Beta open sites has been performed using periodic-DFT, to enable a comparison of open site stability on equal footing. This communication closes that gap by comparing the energies of 144 distinct Sn-Beta open sites, as well as the binding and spectroscopic features of the most stable sites that are identified.

## 2. Electronic structure methods

Periodic density function theory calculations were performed using the GPAW software [27,28] in the ASE framework [29]. The core electrons were represented with the PAW formalism [30,31], while the valence electrons were represented with the Perdew-Burke-Ernzerhof (PBE) exchange-correlation functional [32]. Optimizations were performed using the quasi-Newton limited memory Broyden–Fletcher–Goldfarb–Shanno (LBFGS) optimizer [33]. Initial optimizations used a double-ζ plus polarization (DZP) linear combination of atomic orbitals (LCAO) basis set [34], and final optimizations were performed using the finite difference approach with a grid spacing of 0.2 Å. Electronic energies were optimized to a precision to $10^{-6}$ eV, with a Fermi-Dirac smearing of 0.1 eV, and nuclear degrees of freedom were optimized to a force convergence threshold of 0.05 eV $Å^{-1}$. Dispersion corrections were estimated using Grimme's DFT-d3 method [35], with structures reoptimized to 0.05 eV $Å^{-1}$. Frequencies and entropic corrections were calculated using LCAO, after re-optimizing with tighter electronic ($10^{-8}$ eV) and force (0.01 eV $Å^{-1}$) convergence thresholds. All calculations were performed at the Γ-point.

## 3. Results and discussion

### 3.1. Relative stability of closed sites

The geometry of polymorph A of the BEA zeolite framework [36] was obtained from the International Zeolite Association online database [37]. Experimental unit cell parameters 12.632 × 12.632 × 26.186 Å were used. Sn atoms were substituted into the framework once at each of the nine T sites, with a Si/Sn ratio of 63 for all structures. The relative stability using PBE and PBE-d3 is reported in Table 1, in addition to those reported by Shetty et al. [20,40].

We find several stable sites for Sn substitution, with T9, T1, and T6 within 1 kcal/mol. In fact, 7 of the sites are within 2.5 kcal/mol of the most stable T9, suggesting there may be a broad distribution of Sn substitutions at multiple sites. These calculations are considerably different from Shetty, et al. [20], who found T2 and T8 to be relatively stable, and Yang, et al. [40], who found T2, T5, and T9 to be relatively stable. Differences between these works arise from differences in pseudopotentials (ultrasoft vanderbilt vs PAW) and in dispersion corrections (DFT-D vs DFT-D3).

### 3.2. Relative stability of open sites

The open site of Sn-Beta occurs through the hydrolysis of the closed Sn site, producing a SnOH and a neighboring SiOH. As depicted in Fig. 1, the closed Sn site is tetrahedral, with four framework bonds (1–4), and four "gaps" opposite each framework bond (A-D). Binding an OH to one of the "gaps" and binding an H to one of the bridges generates an open site. Each of the nine T sites has four "gaps" and four bridges, generating 144 unique geometries. For the most stable geometries, the SiOH and SnOH were rotated and reoptimized to search for the most stable configuration.

The BEA framework has two 12-ring cylindrical channels along the a and b directions, and a helical channel intersecting these along the c direction. Smaller 4, 5, and 6-ring channels also extend through the a and b directions, forming small (4 and 5-ring) and medium (6-ring) pockets between the 12-ring channels. For this study, we have organized the sites according to the location of each "gap" for the OH in a channel, medium cage, or small cage, and the connectivity of each bridge for the H (details available in the Supporting Information). In our geometry nomenclature, T1-O12A indicates a Sn at position T1, with the hydrogen on the oxygen of the T1-T2 bridge, and with the OH in gap A, a channel according to Table S1.

From this survey, we find the most stable open site to be T9-O29B, depicted in Fig. 2 along with a couple less stable alternative geometries (coordinates for these, and all other structures are included as Supporting Information). This site is characterized by a SnOH protruding into a channel, and the hydrolyzed bridge opposite the SnOH, so the SiOH oxygen is stabilized by the Sn. In fact, the most stable geometry for each site (highlighted in bold in Table S2), is always characterized in the same way – the SnOH in a channel and the SiOH behind the SnOH.

In Fig. 3, the full data is plotted against a geometric descriptor: the distance between the oxygen atom of SnOH and the hydrogen atom of SiOH. This reveals a distinct pattern in the possible geometries: when the SiOH is behind the SnOH, the O···H distance is greater than 4 Å; hydrolyzing any of the other three bridges results in a shorter O···H distance. Moreover, the relative stability of the long-distance geometries over the short-distance ones is clear by comparing energies of structures within the same T site.

### 3.3. Possible formation mechanisms for open site formation

Sn-Beta synthesis starts from dealuminated H-Beta. Removing aluminum leaves behind silanol "nests," which react with $SnCl_4$ as it is incorporated into the framework. Incomplete condensation of all the silanols could generate open sites. The dynamics of this process are outside the scope of this paper, but one can imagine the possibility of open sites with either "adjacent" or "opposite" configurations after condensation. As we have shown, open sites with the SiOH adjacent to the SnOH are typically thermodynamically less stable than those with the SiOH opposite the SnOH. In some of these cases (but not all), the adjacent SiOH can transfer its proton to the opposite Sn-O-Si bridge and form the corresponding opposite open site. We tested this for converting T9-O49A (adjacent SiOH) into T9-O29A (opposite SiOH) and found the proton transfer to have a negligible barrier (11 kcal/mol) for relaxing to the more stable open site geometry. Alternatively, water can assist the proton

[1] Note about T site nomenclature: Here, we use the nomenclature originating in the work by Newsam et al. [36] and Valerio et al. [38] An alternative nomenclature is used by the International Zeolite Association Structure Commission website. We have included a note in the Supporting Information for clarification.

**Table 1**
Relative stability of closed Sn-Beta sites

| | ΔE, PBE, kcal/mol | ΔE, PBE-d3, kcal/mol | ΔE from Shetty, et al.[20] (kcal/mol) | ΔE from Yang, et al.[40] (kcal/mol) |
|---|---|---|---|---|
| T1 | 0.459 | 1.074 | 6.762 | 2.39 |
| T2 | 2.198 | 2.767 | 0 | 0 |
| T3 | 1.386 | 1.347 | 4.899 | 2.39 |
| T4 | 1.761 | 2.162 | 3.634 | 3.11 |
| T5 | 4.013 | 4.338 | 6.348 | 0.96 |
| T6 | 0.866 | 1.172 | 5.750 | 1.91 |
| T7 | 2.802 | 3.086 | 5.152 | 3.35 |
| T8 | 2.273 | 1.876 | 1.380 | 1.67 |
| T9 | 0 | 0 | 8.234 | 0.96 |

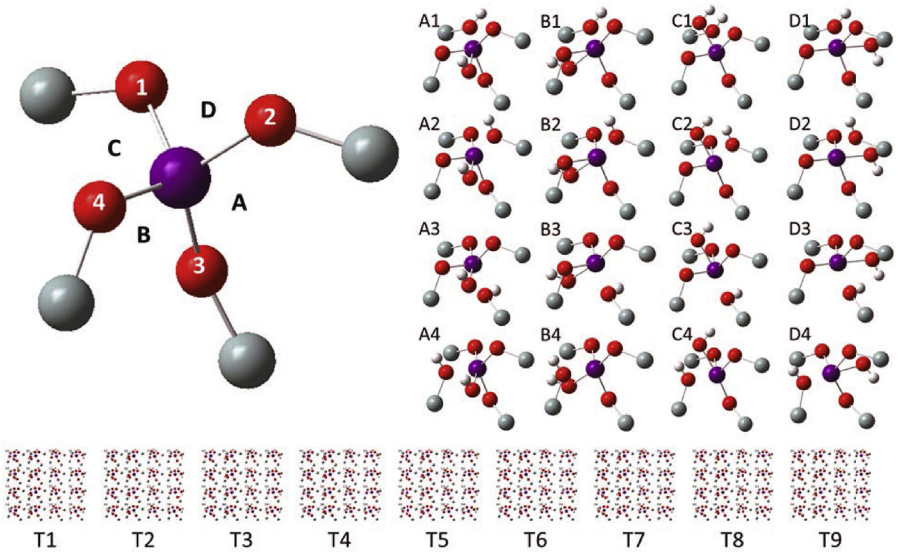


**Fig. 1.** Diagram depicting tetrahedral Sn site, and four framework bonds (1–4) and four "gaps" opposite each framework bond (A–D). To form an open site, one H is placed on a framework bond and one OH is placed in a "gap," providing 16 unique bonding patterns for each T site. Repeating this procedure on all nine T sites generates 144 candidate open sites.

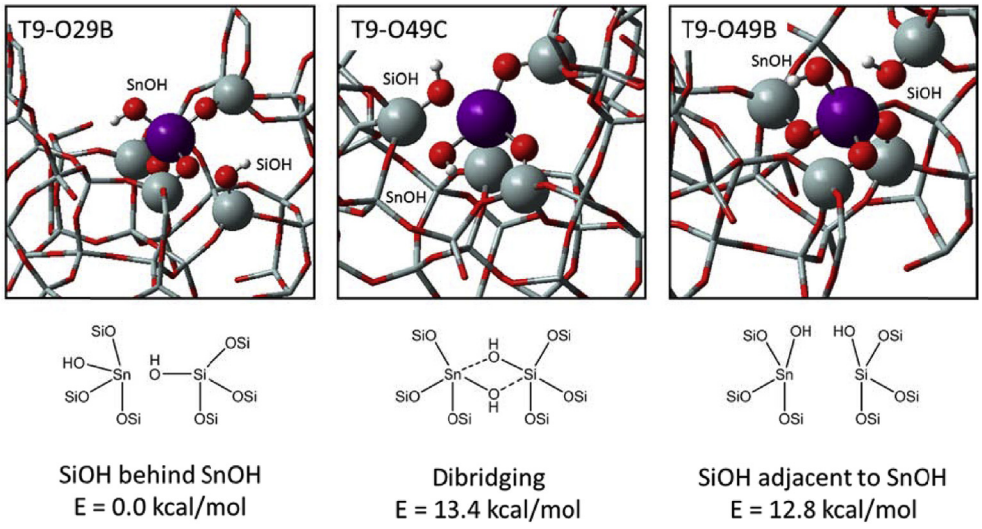


**Fig. 2.** Selected geometries of different open site configurations. T9-O29B is the most stable open site geometry, and the SiOH is positioned behind the SnOH. Two additional geometries, T9-O49C and T9-O49B are shown to illustrate examples of less stable dibridging and H-bonded open sites, respectively. Energies are reported with respect to the most stable T9-O29B geometry.

transfer through the Grotthuss mechanism, reducing this already-small barrier to 1 kcal/mol (Table S3).

Another hypothesized route is through the hydrolysis of closed sites. After adsorption to a closed site, water deprotonates to a Sn-

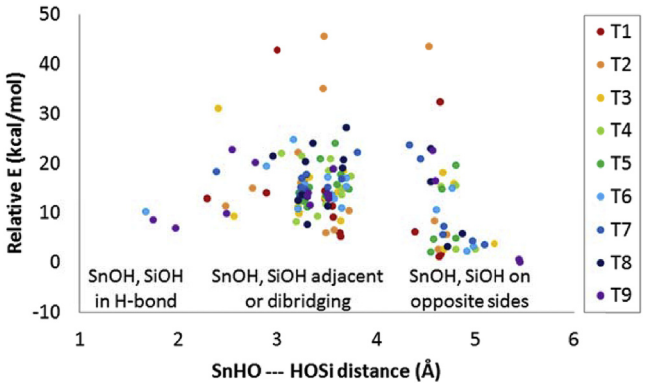


**Fig. 3.** Relative PBE energy (kcal/mol) of open sites with respect to the distance between the oxygen of SnOH and the hydrogen of SiOH. The largest O–H distances (>4 Å) correspond to geometries in which the SnOH and SiOH are on opposite sides, the shortest distances (<2 Å) are approximate H-bonds between SiOH and SnOH, and the intermediate distances include the other structures, including the dibridging geometries.

O-Si bridge, forming an "adjacent" open site. Rotation of the H atom about the Si-O bond can then direct it toward the Sn-O-Si bridge that is opposite the SnOH. Transfer of the proton from the SiOH to the bridge could then generate the "opposite" open site. For converting the T9 closed site into T9-O29A in the gas phase, we found the overall barrier to be 24.6 kcal/mol. Details of the reaction are provided in Table S3 in the Supporting Information.

### 3.4. Adsorption of Lewis bases

Adsorption energies of the Lewis bases $NH_3$, pyridine, and acetonitrile were also calculated for the most stable closed (T9) and open site (T9-O29B) geometries (Table 2 and Fig. 4). Because the Sn site is at the intersection of two channels, adsorbates can coordinate to two locations on the Sn closed and open sites, as well as to the SnOH and the SiOH for the open site. Different features of the active sites strongly affect adsorption behavior. For all systems, with the exception of $NH_3$ with PBE-d3, the open site binds 2.5–8 kcal/mol more strongly than the closed site, in agreement with prior work [15].

Acetonitrile binds more weakly to the sites than $NH_3$ and pyridine. It binds most strongly to the Sn Lewis acid of the open site, binding 2–4 kcal/mol more weakly to the Sn closed site or to the SnOH or SiOH. For the stronger bases, $NH_3$ and pyridine, the SnOH is weakly binding, while the Sn Lewis acid binds comparably to the SiOH; for PBE, the Sn Lewis acid binds 2–3 kcal/mol more strongly that the SiOH, while for PBE-d3, the SiOH binds 1–2 kcal/mol more strongly than the Sn Lewis acid. IR spectroscopy of Sn-Beta with adsorbed pyridine has not shown evidence of pyridinium, possibly indicating that pyridine adsorption to the Lewis site is favored over adsorption to the SiOH, in agreement with the PBE binding energies, but not the PBE-d3 [17].

Adsorption geometries (PBE) are shown in Fig. 4. These highlight the unusually acidic nature of the SiOH in the Sn-Beta open site. For $NH_3$ and pyridine, the SiOH deprotonates to the adsorbate, and the SiO binds to the Sn. In the open site, the Sn···O(H)Si distance is 3.23 Å, while the SiO···H distance is 0.98 Å. When $NH_3$ or pyridine bind to the SiOH, the Sn···O(H)Si distances shrinks to 2.16 Å and 2.14 Å, respectively, and the SiO···H distance increases to 1.60 and 1.80 Å, respectively. Acetonitrile does not abstract the proton, leaving the SiO···H distance at 1.02 Å, but the Sn···O(H)Si distance still decreases to 2.48 Å, indicating some stabilization of the SiOH by the Sn.

### 3.5. Acetonitrile vibrations

We calculated vibrational frequencies for adsorbed acetonitrile to compare with prior work (see Table 3). The $\nu$(C≡N) frequency blueshifts as acetonitrile binds to the catalyst, and it shifts by 35.5 $cm^{-1}$ on the closed Sn site, and 41.2 $cm^{-1}$ on the open Sn site, the same trend observed in cluster models of closed and open sites [15], and in agreement with experimental shifts of the peaks assigned to these two types of Lewis sites [1,14,15].

Acetonitrile can also bind to the SnOH and the SiOH in the open site. Adsorption to the SnOH shifts $\nu$(C≡N) by 13 $cm^{-1}$, while adsorption to the SiOH shifts $\nu$(C≡N) significantly more; by 29.6 $cm^{-1}$. To compare this to SiOH defects and surface SiOH, we created a SiOH defect in the Sn-Beta framework by replacing the Sn in the open site with a Si, and also by removing the Sn atom. Acetonitrile binds less strongly to these SiOH groups, with $\nu$(C≡N) shifting by an average of 18.2 $cm^{-1}$. The trend in these shifts on these typical SiOH groups is consistent with experimental $\nu$(C≡N) shift of 10 $cm^{-1}$, as well as calculated $\nu$(C≡N) shift for a bare SiOH cluster [15]. Boronat et al. found the calculated frequency for SnOH binding to be comparable to that of SiOH, in agreement with our calculated $\nu$(C≡N) shift on the SnOH. However, the open site SiOH next to the Sn is significantly more acidic, with a dramatically stronger $\nu$(C≡N) compared to a surface SiOH, indicative of its unique character because of its interaction with the Sn. This Brønsted acidity, arising from the Sn···O(H)Si interaction in the hydrolyzed open site, is consistent with experimental IR spectroscopy of adsorbed $CD_3CN$ [1,2], and with observations of etherification activity in Sn-Beta [12].

## 4. Conclusions

Using periodic DFT, we have completed a survey of open site geometries in the Sn-Beta zeolite. At every T site, the most stable geometry is characterized by a SnOH protruding into a channel, and an SiOH behind the SnOH. The most stable site is the T9, although

**Table 2**
Binding energies in kcal/mol calculated with PBE for various bases on the Sn sites, with gas phase adsorbate and bare catalyst as reference.

| | Closed Sn 1 | Closed Sn 2 | Open Sn 1 | Open Sn 2 | SnOH | SiOH |
|---|---|---|---|---|---|---|
| PBE ΔE | | | | | | |
| Acetonitrile | −7.00 | −6.98 | −9.56 | −10.43 | −8.55 | −6.13 |
| $NH_3$ | −15.54 | −16.11 | −15.72 | −18.49 | −10.36 | −15.45 |
| Pyridine | −12.47 | −12.06 | −13.90 | −20.91 | −9.12 | −18.40 |
| PBE-d3 ΔE | | | | | | |
| Acetonitrile | −15.98 | −16.01 | −17.39 | −16.01 | −14.33 | −14.40 |
| $NH_3$ | −21.46 | −22.20 | −21.09 | −21.85 | −13.82 | −22.24 |
| Pyridine | −27.73 | −27.36 | −29.21 | −32.35 | −22.41 | −34.34 |
| PBE ΔG | | | | | | |
| Acetonitrile | 6.33 | | 1.01 | −2.55 | 0.08 | 4.13 |

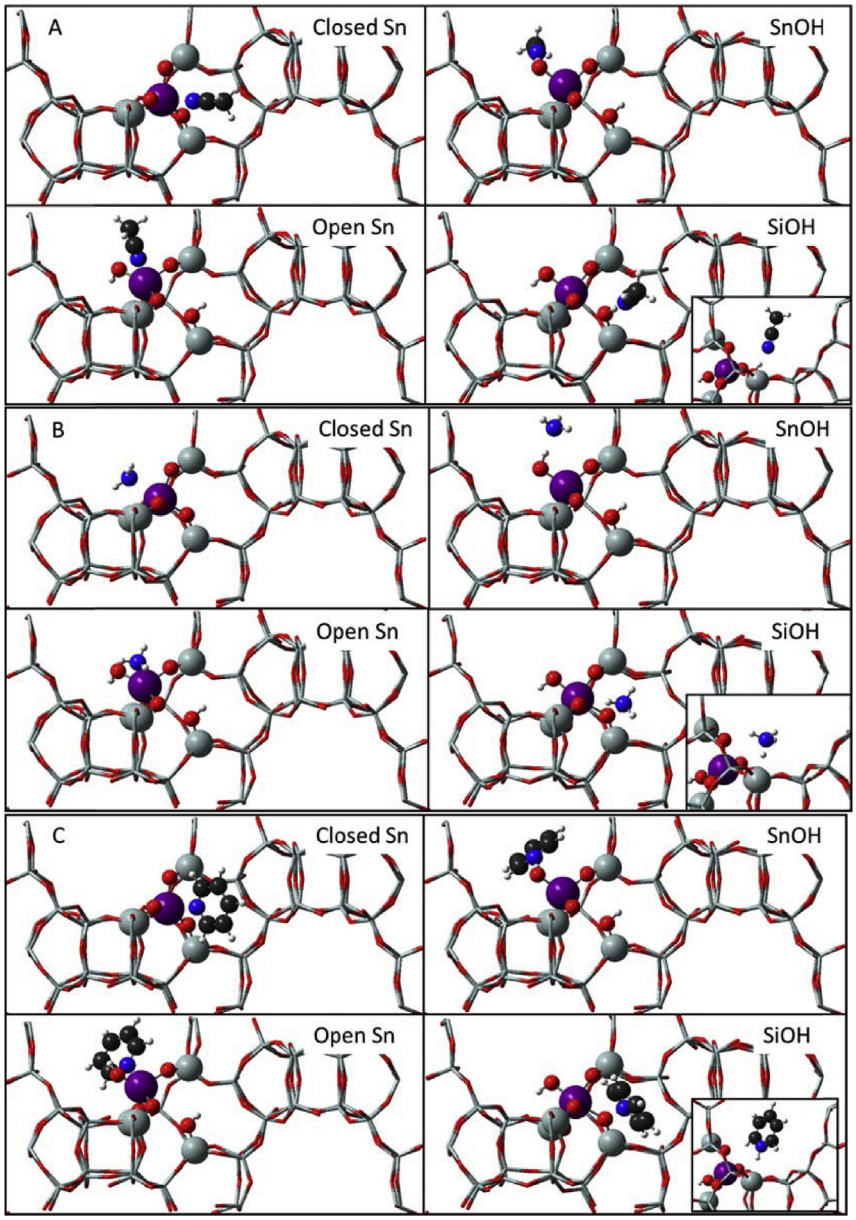


**Fig. 4.** Most stable adsorption geometries of acetonitrile (A), $NH_3$ (B), and pyridine (C) on the T8 Sn-Beta closed Sn site, open Sn site, open SnOH, and open SiOH. Inset image shows side view of adsorbate bound to the SiOH. Adsorbates and first coordination shell around Sn site are depicted using ball-and-stick model, while rest of zeolite framework is depicted using tube model.

several T sites have energies within 2 kcal/mol of the most stable geometry. Adsorption of strong bases such as $NH_3$ and pyridine is favored at the open Sn Lewis site; however adsorption to the SiOH has comparable binding strength to the Lewis site, and resulted into

**Table 3**
Vibrational frequencies of acetonitrile adsorbed onto different Sn sites, and comparison with literature. *Harris et al. [1] assigned this frequency to a speculated doubly-hydrolyzed Sn site and Otomo et al. [2] observed this peak, but did not assign it; we list it here with our proposed assignment.

| | Closed Sn | Open Sn | Open Sn SiOH (acidic) | Open Sn SiOH | SnOH | SiOH | Gas Phase |
|---|---|---|---|---|---|---|---|
| Calc. $\nu$(C≡N) ($cm^{-1}$) | 2281.9 | 2287.6 | 2278.2 | 2261.7 | 2261.6 | 2266.8 | 2248.6 |
| $\Delta\nu$(C≡N) ($cm^{-1}$) | 33.3 | 39 | 29.6 | 13.1 | 13.0 | 18.2 | 0 |
| Exp [15]. $\nu$(C≡N) ($cm^{-1}$) | 2308 | 2316 | | | | 2276 | 2265 |
| $\Delta\nu$(C≡N) ($cm^{-1}$) | 43 | 51 | | | | 11 | 0 |
| Calc [15]. $\Delta\nu$(C≡N) ($cm^{-1}$) Average of T1, T5, T9 | 43 | 53 | | | 17 | 16 | |
| Exp [14]. $\nu$(C≡N) ($cm^{-1}$) $\Delta\nu$(C≡N) ($cm^{-1}$) | 2307 | 2315 | | | | 2276 | |
| Exp [1,2]. $\nu$(C≡N) ($cm^{-1}$) | 2308 | 2316 | 2287* | | | 2275 | 2265 |
| $\Delta\nu$(C≡N) ($cm^{-1}$) | 43 | 51 | 22* | | | 10 | 0 |

abstraction of the SiOH proton. Calculated frequency shifts of acetonitrile are in agreement with prior experimental and theoretical work. The primary finding is evidence for unusual Brønsted acidity in the Sn-Beta open site, which may enable new reaction mechanisms not yet considered in the literature.

## Acknowledgements

Research was supported as part of the Catalysis Center for Energy Innovation, an Energy Frontier Research Center funded by the U.S. Department of Energy (DOE), Office of Science, Basic Energy Sciences (BES), under Award number DE-SC0001004. This research used resources of the National Energy Research Scientific Computing Center, a DOE Office of Science User Facility supported by the Office of Science of the U.S. Department of Energy under Contract No. DE-AC02-05CH11231. T.R.J. wishes to acknowledge funding from the National Science Foundation Graduate Research Fellowship Program under Grant No. 0750966, as well as the George W. Laird Merit Fellowship. Any opinions, findings, and conclusions or recommendations expressed in this material are those of the author(s) and do not necessarily reflect the views of the National Science Foundation. The authors would like to thank Zhiqiang Zhang for numerous useful conversations.

## Appendix A. Supplementary data

Supplementary data associated with this article can be found in the online version, at http://dx.doi.org/10.1016/j.micromeso.2017.02.065. These data include MOL files and InChiKeys of the most important compounds described in this article.

## References

[1] J.W. Harris, M.J. Cordon, J.R. Di Iorio, J.C. Vega-Vila, F.H. Ribeiro, R. Gounder, J. Catal. 335 (2016) 141–154.
[2] R. Otomo, R. Kosugi, Y. Kamiya, T. Tatsumi, T. Yokoi, Catal. Sci. Technol. 6 (2016) 2787–2795.
[3] A. Corma, L.T. Nemeth, M. Renz, S. Valencia, Nature 412 (2001) 423–425.
[4] A. Corma, M.E. Domine, L. Nemeth, S. Valencia, J. Am. Chem. Soc. 124 (2002) 3194–3195.
[5] M. Moliner, Y. Roman-Leshkov, M.E.E. Davis, Y. Román-Leshkov, M.E.E. Davis, Proc. Natl. Acad. Sci. U. S. A. 107 (2010) 6164–6168.
[6] V. Choudhary, A.B. Pinar, S.I. Sandler, D.G. Vlachos, R.F. Lobo, ACS Catal. 1 (2011) 1724–1728.
[7] M.S. Holm, S. Saravanamurugan, E. Taarning, Science 328 (2010) 602–605.
[8] M. Orazov, M.E. Davis, Proc. Natl. Acad. Sci. U. S. A. 112 (2015) 201516466.
[9] R. Bermejo-Deval, R. Gounder, M.E. Davis, ACS Catal. 2 (2012) 2705–2713.
[10] W.R. Gunther, Y. Wang, Y. Ji, V.K. Michaelis, S.T. Hunt, R.G. Griffin, Y. Román-Leshkov, Nat. Commun. 3 (2012) 1109.
[11] C.L. Williams, C.-C. Chang, P. Do, N. Nikbin, S. Caratzoulas, D.G. Vlachos, R.F. Lobo, W. Fan, P.J. Dauenhauer, ACS Catal. 2 (2012) 935–939.
[12] J.D. Lewis, S. Van De Vyver, A.J. Crisci, W.R. Gunther, V.K. Michaelis, R.G. Griffin, Y. Román-Leshkov, ChemSusChem 7 (2014) 2255–2265.
[13] R. Bermejo-Deval, R.S.S. Assary, E. Nikolla, M. Moliner, Y. Román-Leshkov, S.-J.S.-J. Hwang, A. Palsdottir, D. Silverman, R.F.F. Lobo, L. a. a. Curtiss, M.E.E. Davis, Y. Roman-Leshkov, S.-J.S.-J. Hwang, A. Palsdottir, D. Silverman, R.F.F. Lobo, L. a. a. Curtiss, M.E.E. Davis, Proc. Natl. Acad. Sci. U. S. A. 109 (2012) 9727–9732.
[14] R. Bermejo-Deval, M. Orazov, R. Gounder, S.J. Hwang, M.E. Davis, ACS Catal. 4 (2014) 2288–2297.
[15] M. Boronat, P. Concepción, A. Corma, M. Renz, S. Valencia, J. Catal. 234 (2005) 111–118.
[16] Y. Zhu, G.K. Chuah, S. Jaenicke, J. Catal. 241 (2006) 25–33.
[17] B. Tang, W. Dai, G. Wu, N. Guan, L. Li, M. Hunger, ACS Catal. 4 (2014) 2801–2810.
[18] S.K. Brand, J.A. Labinger, M.E. Davis, ChemCatChem 8 (2016) 121–124.
[19] S.K. Brand, T.R. Josephson, J.A. Labinger, S. Caratzoulas, D.G. Vlachos, M.E. Davis, J. Catal. 341 (2016) 62–71.
[20] S. Shetty, S. Pal, D.G. Kanhere, A. Goursot, Chem. A Eur. J. 12 (2005) 518–523.
[21] S.R. Bare, S.D. Kelly, W. Sinkler, J.J. Low, S. Valencia, A. Corma, L.T. Nemeth, F.S. Modica, S. Valencia, A. Corma, L.T. Nemeth, J. Am. Chem. Soc. 127 (2005) 12924–12932.
[22] G. Yang, E.A. Pidko, E.J.M. Hensen, ChemSusChem 6 (2013) 1688–1696.
[23] Y.P.P. Li, M. Head-Gordon, A.T.T. Bell, ACS Catal. 4 (2014) 1537–1545.
[24] T.D. Courtney, C.-C. Chang, R.J. Gorte, R.F. Lobo, W. Fan, V. Nikolakis, Microporous Mesoporous Mater. 210 (2015) 69–76.
[25] J.R. Christianson, S. Caratzoulas, D.G. Vlachos, ACS Catal. 5 (2015) 5256–5263.
[26] N. Rai, S. Caratzoulas, D.G. Vlachos, ACS Catal. 3 (2013) 2294–2298.
[27] J. Mortensen, L. Hansen, K. Jacobsen, Phys. Rev. B 71 (2005) 35109.
[28] J. Enkovaara, C. Rostgaard, J.J. Mortensen, J. Chen, M. Dułak, L. Ferrighi, J. Gavnholt, C. Glinsvad, V. Haikola, H.A. Hansen, H.H. Kristoffersen, M. Kuisma, A.H. Larsen, L. Lehtovaara, M. Ljungberg, O. Lopez-Acevedo, P.G. Moses, J. Ojanen, T. Olsen, V. Petzold, N.A. Romero, J. Stausholm-Møller, M. Strange, G.A. Tritsaris, M. Vanin, M. Walter, B. Hammer, H. Häkkinen, G.K.H. Madsen, R.M. Nieminen, J.K. Nørskov, M. Puska, T.T. Rantala, J. Schiøtz, K.S. Thygesen, K.W. Jacobsen, J. Phys. Condens. Matter 22 (2010) 253202.
[29] S.R. Bahn, K.W. Jacobsen, Comput. Sci. Eng. 4 (2002) 56–66.
[30] P.E. Blöchl, Phys. Rev. B 50 (1994) 17953–17979.
[31] G. Kresse, Phys. Rev. B 59 (1999) 1758–1775.
[32] J.P. Perdew, K. Burke, M. Ernzerhof, Phys. Rev. Lett. 77 (1996) 3865–3868.
[33] D.C. Liu, J. Nocedal, Math. Program. B 45 (1989) 503–528.
[34] A.H. Larsen, M. Vanin, J.J. Mortensen, K.S. Thygesen, K.W. Jacobsen, Phys. Rev. B Condens. Matter Mater. Phys. 80 (2009) 1–10.
[35] S. Grimme, J. Antony, S. Ehrlich, H. Krieg, J. Chem. Phys. 132 (2010).
[36] J.M. Newsam, M.M.J. Treacy, W.T. Koetsier, C.B. de Gruyter, Proc. R. Soc. Lond. A 420 (1988) 375–405.
[37] C. Baerlocher, L.B. McCusker, Database of Zeolite Structures: http://www.iza-structure.org/databases/.
[38] G. Valerio, A. Goursot, R. Vetrivel, O. Malkina, V. Malkin, D.R. Salahub, J. Am. Chem. Soc. 120 (1998) 11426–11431.
[39] T.R. Josephson, S.K. Brand, S. Caratzoulas, D.G. Vlachos, ACS Catal. 7 (1) (2017) 25–33.
[40] G. Yang, E.A. Pidko, E.J.M. Hensen, J Phys Chem C. 117 (2013) 3976–3986, http://dx.doi.org/10.1021/jp310433r.